Supporting Information

Insight into the Fracture Energy Dissipation Mechanism in Elastomer Composites via Sacrificial bonds and Fillers

Dongyi He [a,b], *Xiaxia Cheng* [a], *Chunyu Wong* [a], *Xiangliang Zeng* [a], *Linling Li* [c], *Chao, Teng* [c,] **, Guoping Du* [b], *Chenxu Zhang* [a,] **, Linlin Ren*[a] , *Xiaoliang Zeng* [a,] ** Rong Sun* [a]

[a]Shenzhen Institute of Advanced Electronic Materials, Shenzhen Institute of Advanced Technology, Chinese Academy of Sciences, Shenzhen 518055, China

[b]School of Physics and Materials Science, Nanchang University, Nanchang 330031, China

[c]Institute of Critical Materials for Integrated Circuits, Shenzhen Polytechnic, Shenzhen, Guangdong 518055

* Authors to whom correspondence should be addressed: tengchao@szpt.edu.cn, cx.zhang@siat.ac.cn, and xl.zeng@siat.ac.cn,

Contents

Supporting Figures

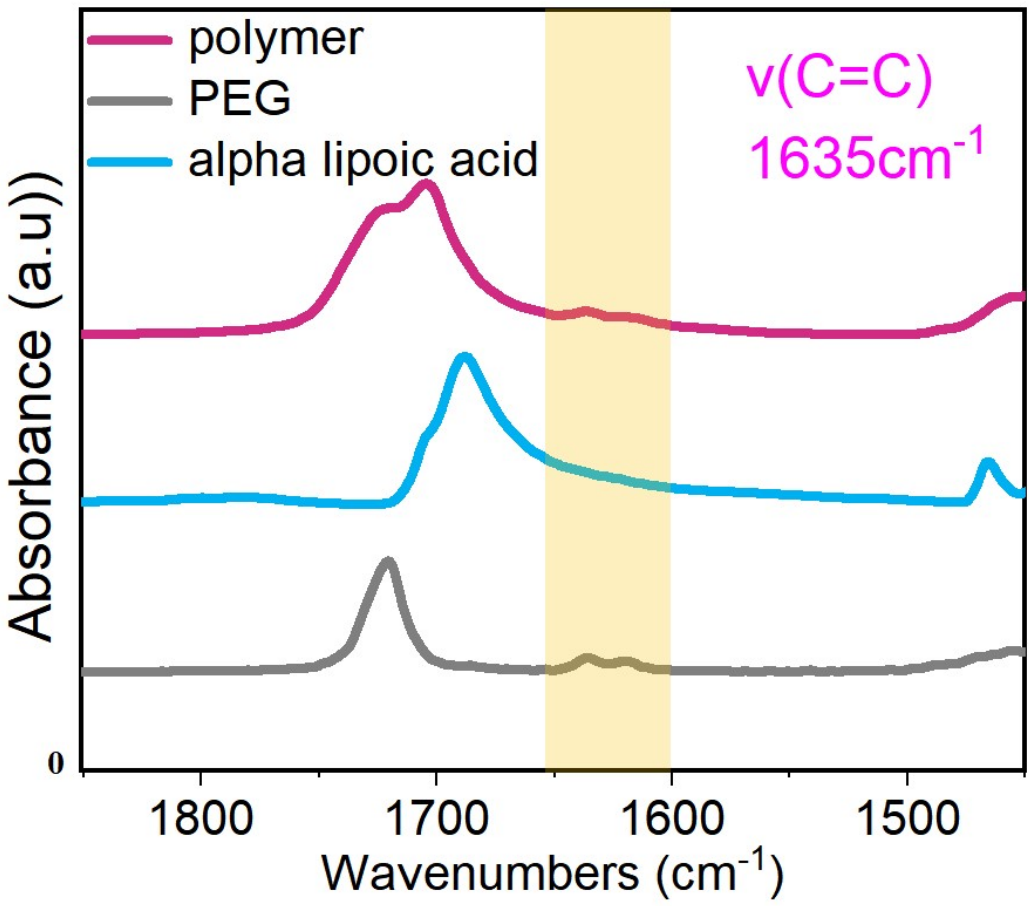

Figure S1. FTIR characterization. The abatement of C=C signal at 1635 cm^{-1}, indicates ring-opening polymerization of lipoic acid, forming the poly (lipoic acid) elastomer.

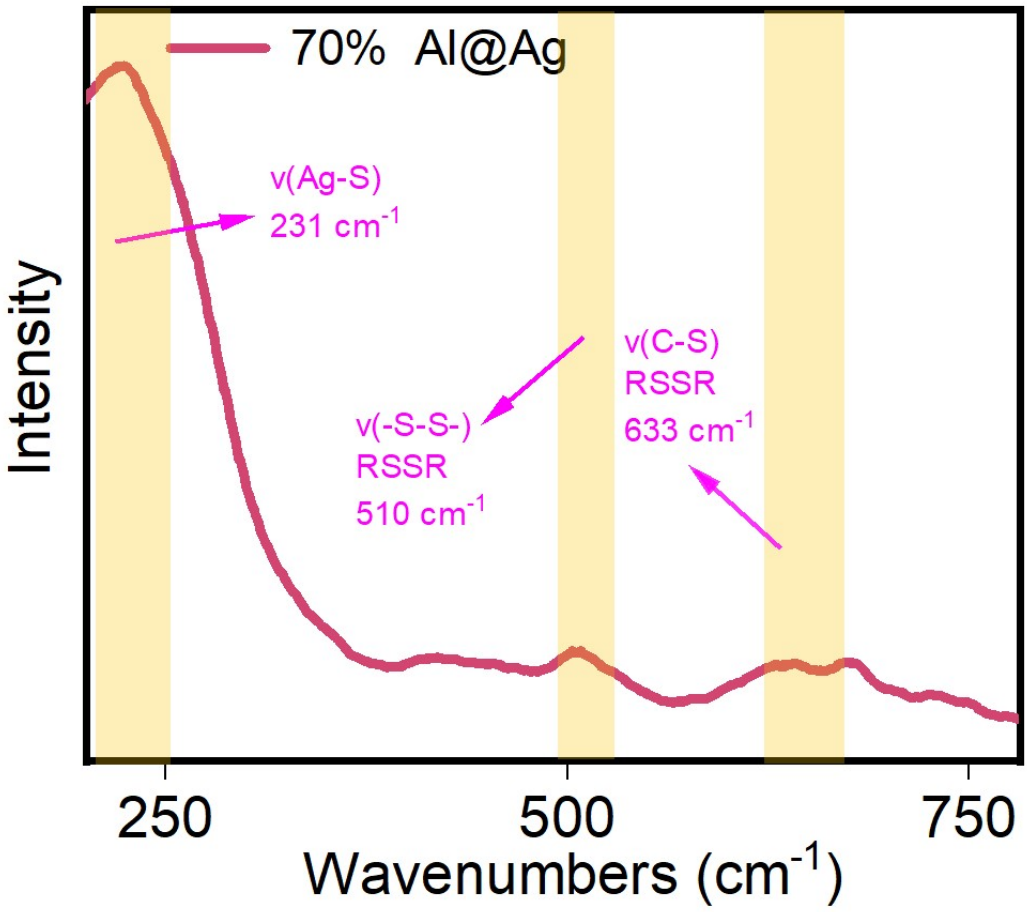

Figure S2. Roman spectrum of the poly (LA)/ 30 vol% Al@Ag.

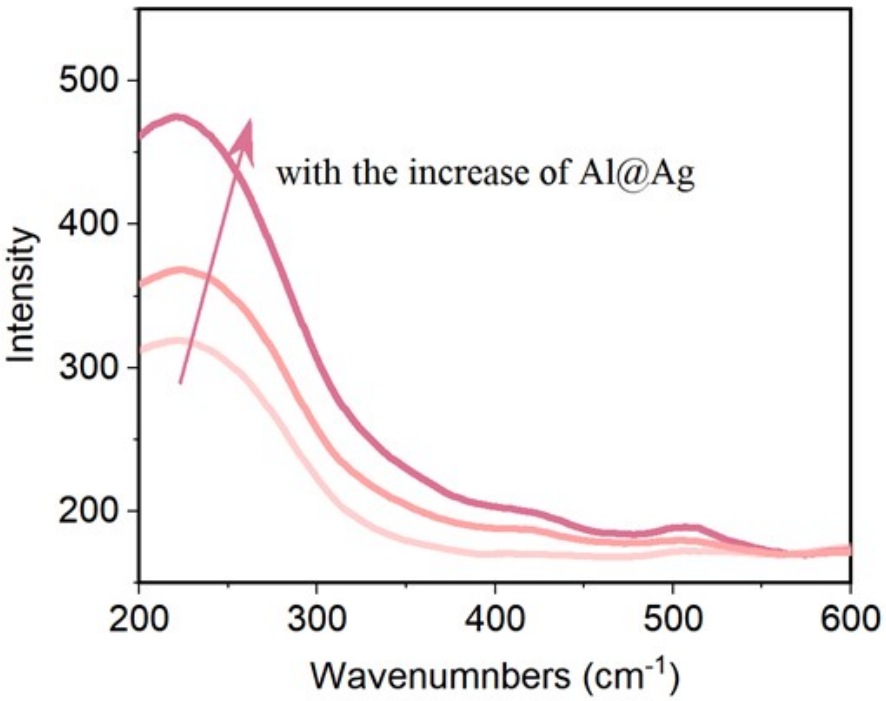

Figure S3. Roman spectrum of elastomers with different content of Al@Ag

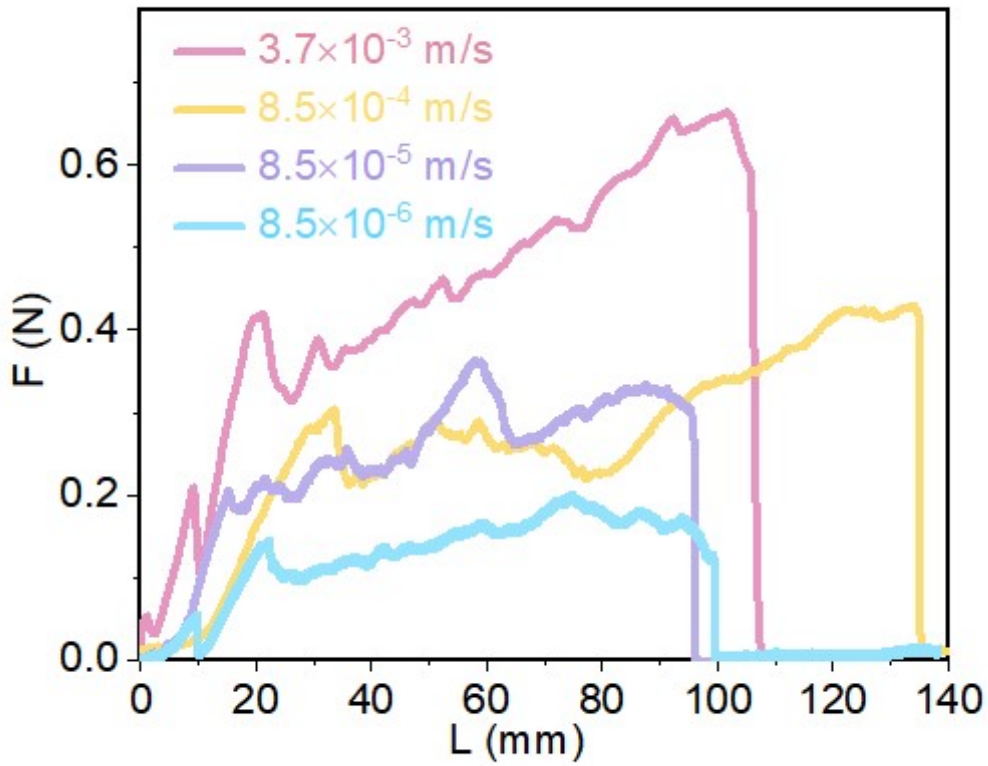

Figure S4. Force−displacement curves of the poly (LA)/Al elastomer composites with different tearing velocities at 25 °C.

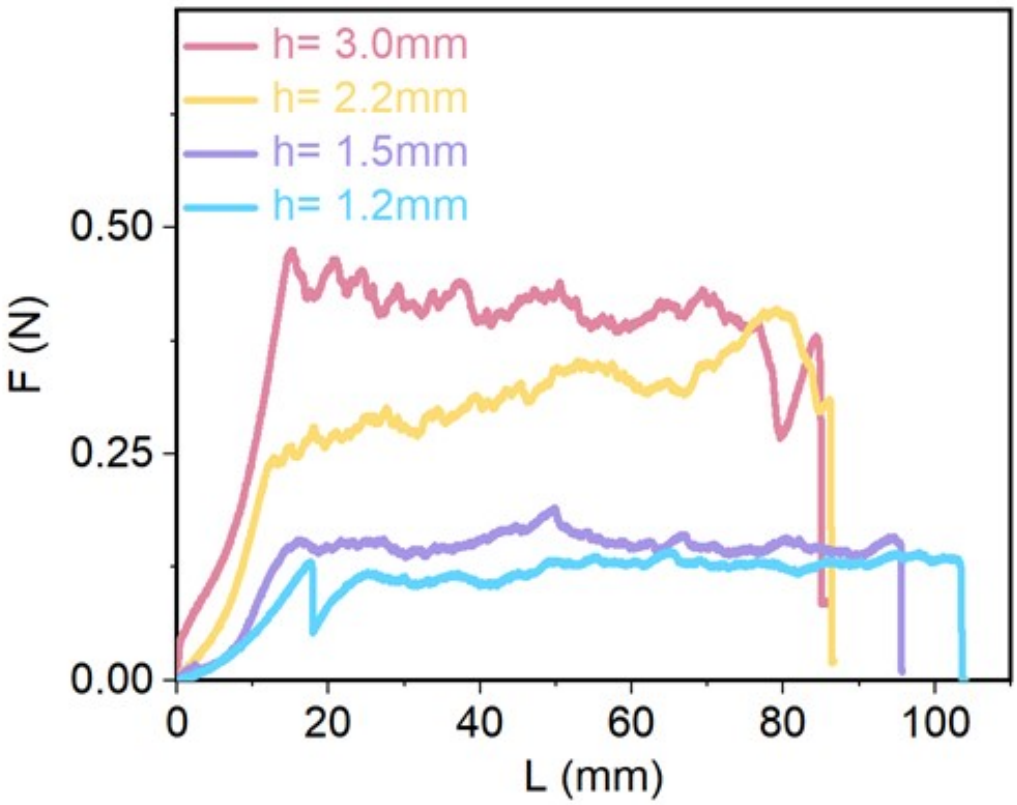

Figure S5. Force−displacement curves of the poly (LA)/Al elastomer composites with 8.5×10-5 m s-1 at 25 °C.

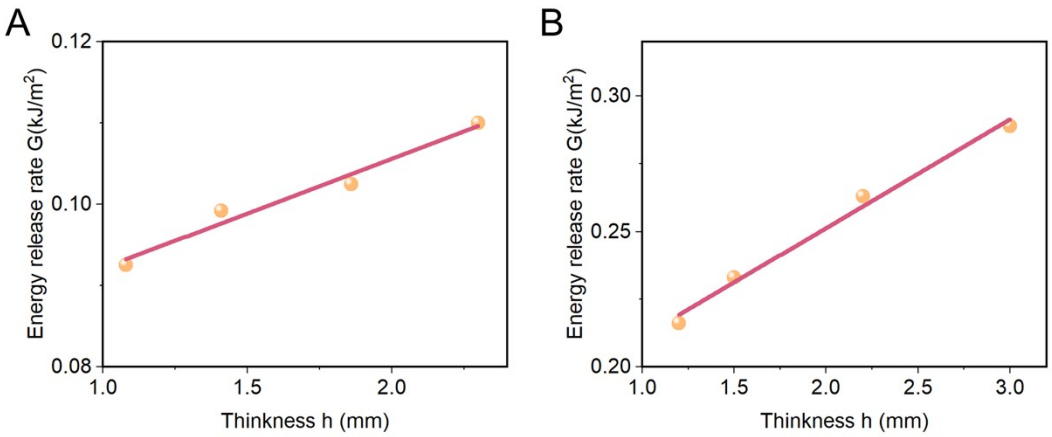

Figure S6. (A) Energy release rate as a function of thickness of the films with 8.5×10^{-5} m s^{-1} of the poly (LA) elastomer. (B) Energy release rate as a function of thickness of the films with 8.5×10^{-5} m s^{-1} of the poly (LA)/Al@Ag elastomer.

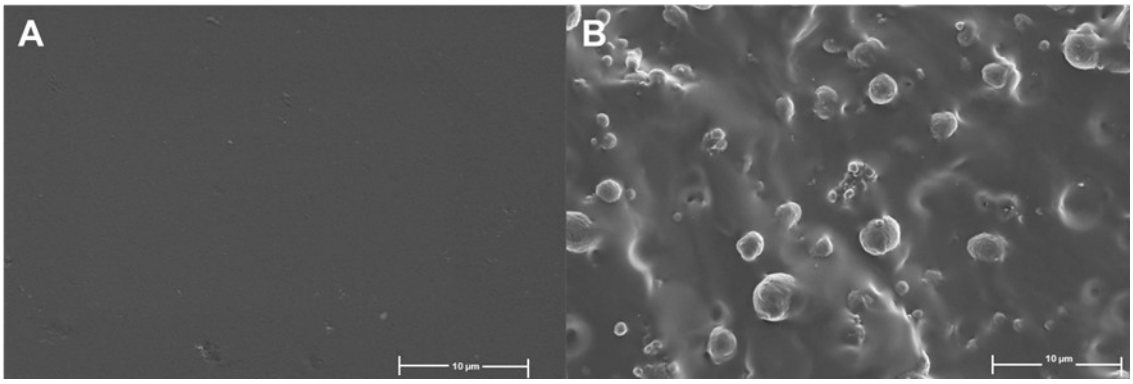

Figure S7. (A) The SEM image of the poly (LA). (B) The SEM image of the poly (LA)/ Al@Ag.

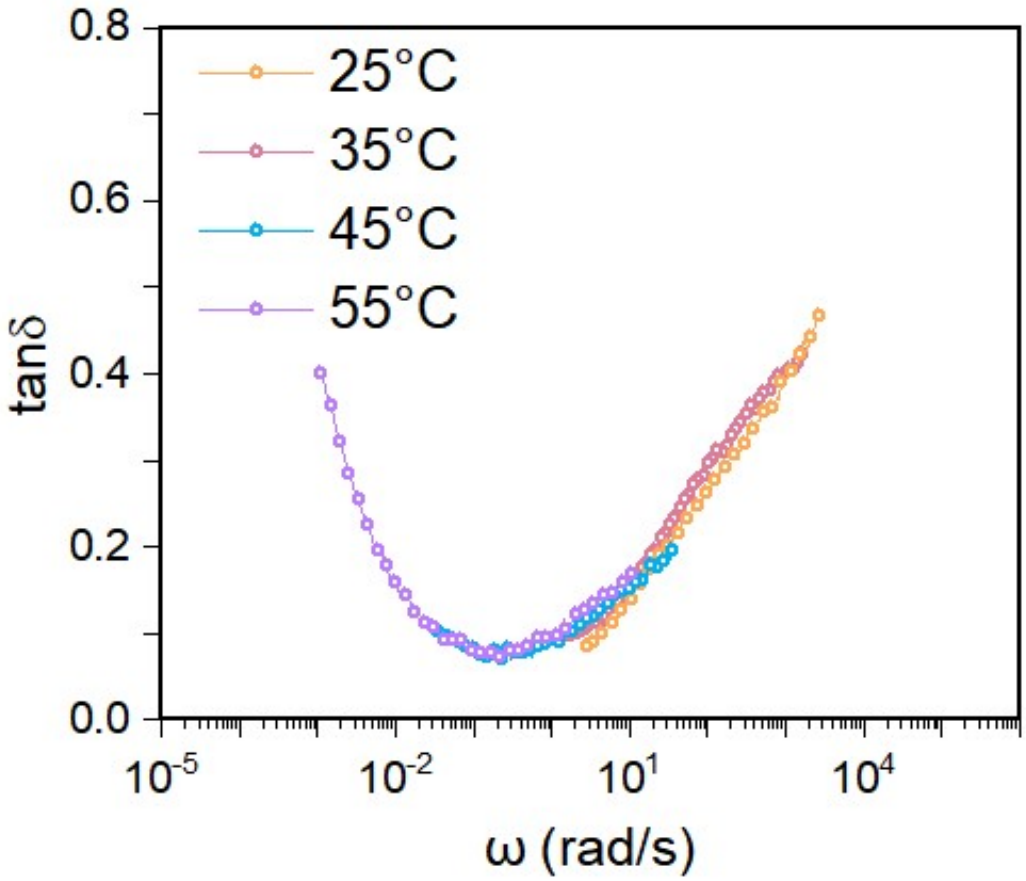

Figure S8. The master curves of loss factor by using the time-temperature superposition of the poly (TA).

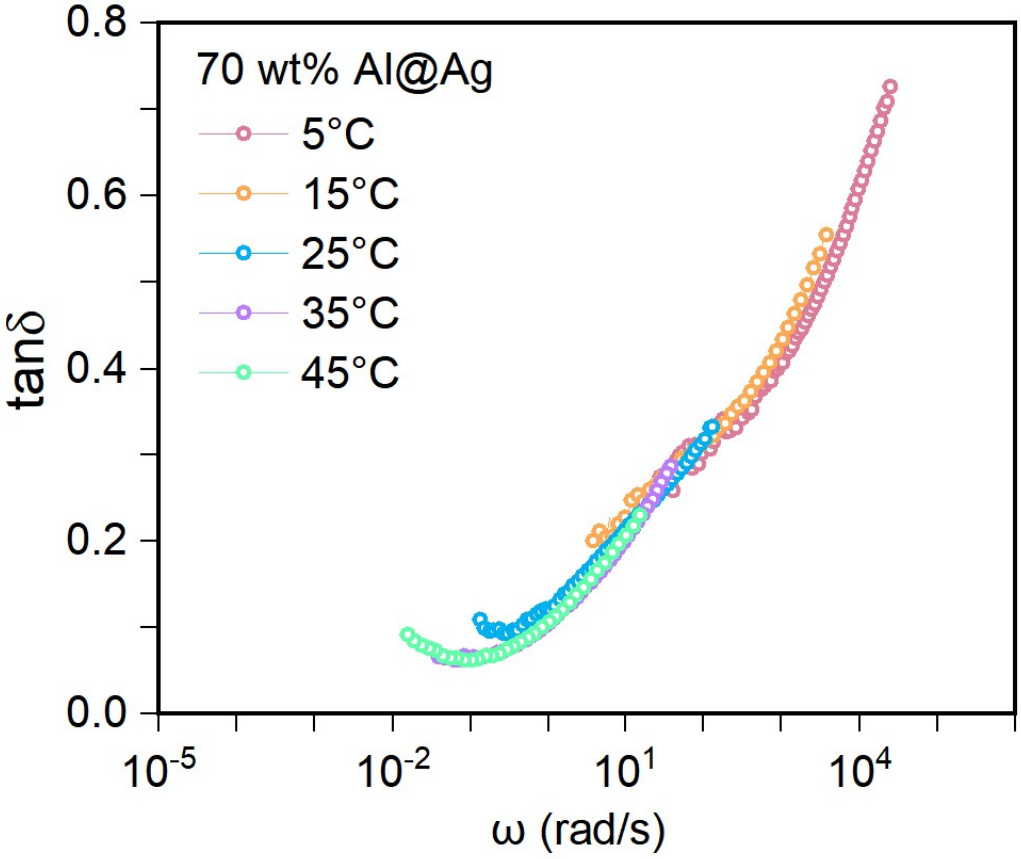

Figure S9. The master curves of loss factor by using the time-temperature superposition of the poly (TA)/Al@Ag.

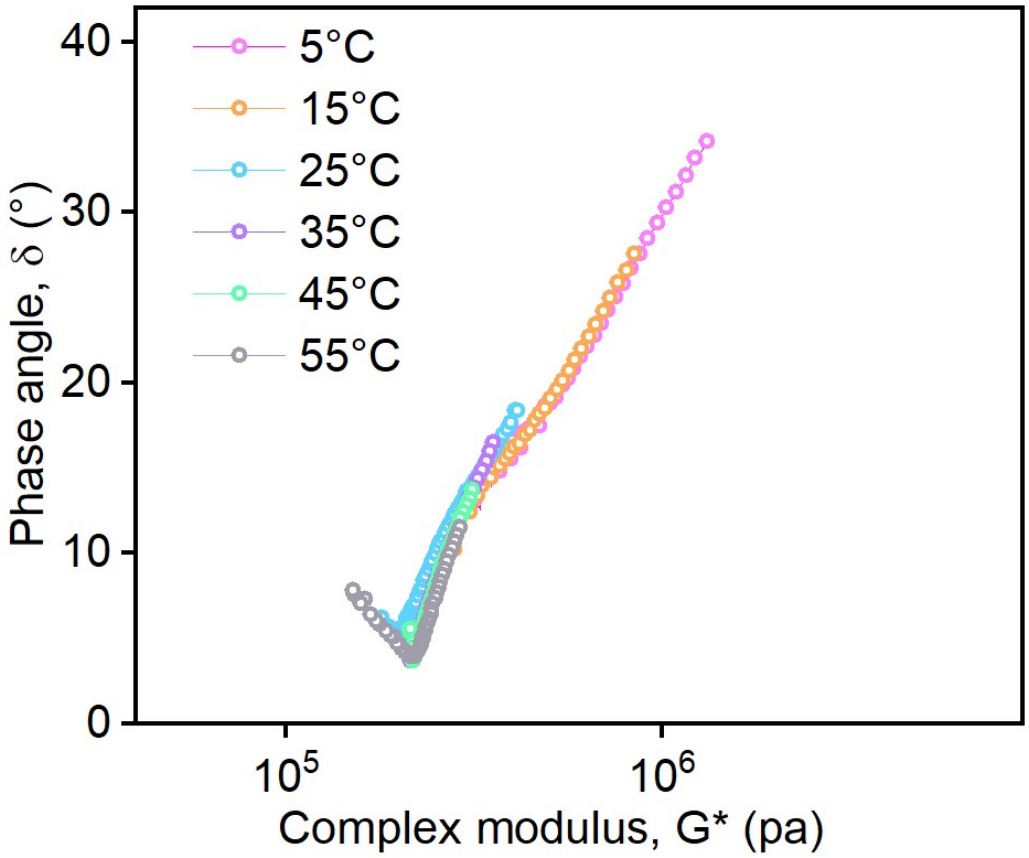

Figure S10. Relationship between the complex modulus G* and phase angle δ of the poly/Al@Ag composites elastomer.

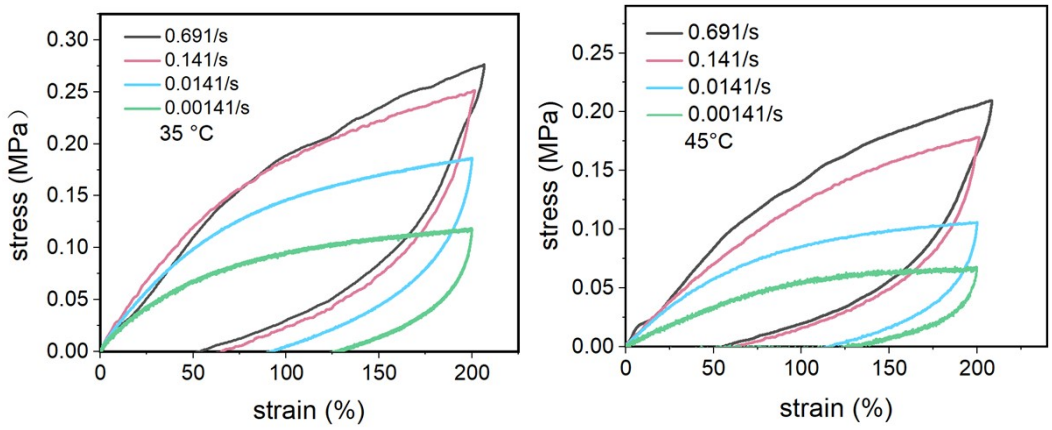

Figure S11. The cyclic stress-strain curves of the poly (LA)/Al@Ag elastomer composites under various stretch strain rate at 35 °C and 45 °C.

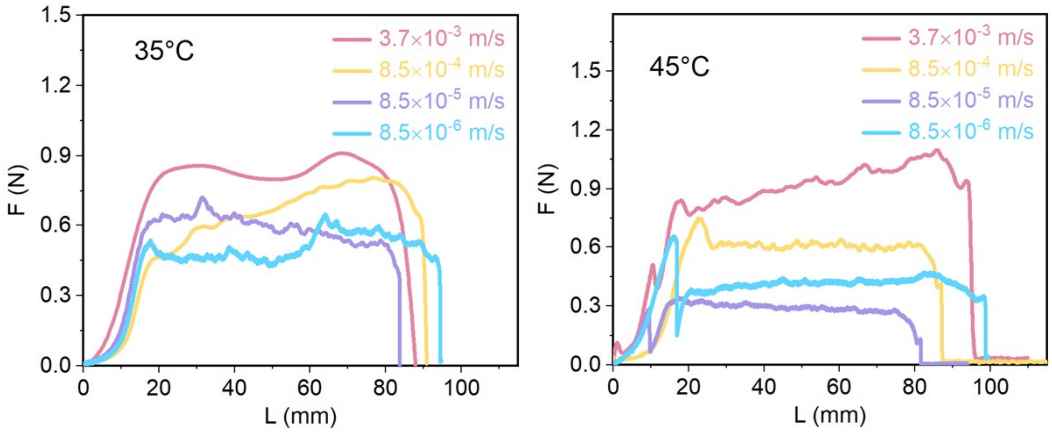

Figure S12. Force−displacement curves of the poly (LA)/Al@Ag elastomer composites with different tearing velocities at 35 °C and 45 °C.

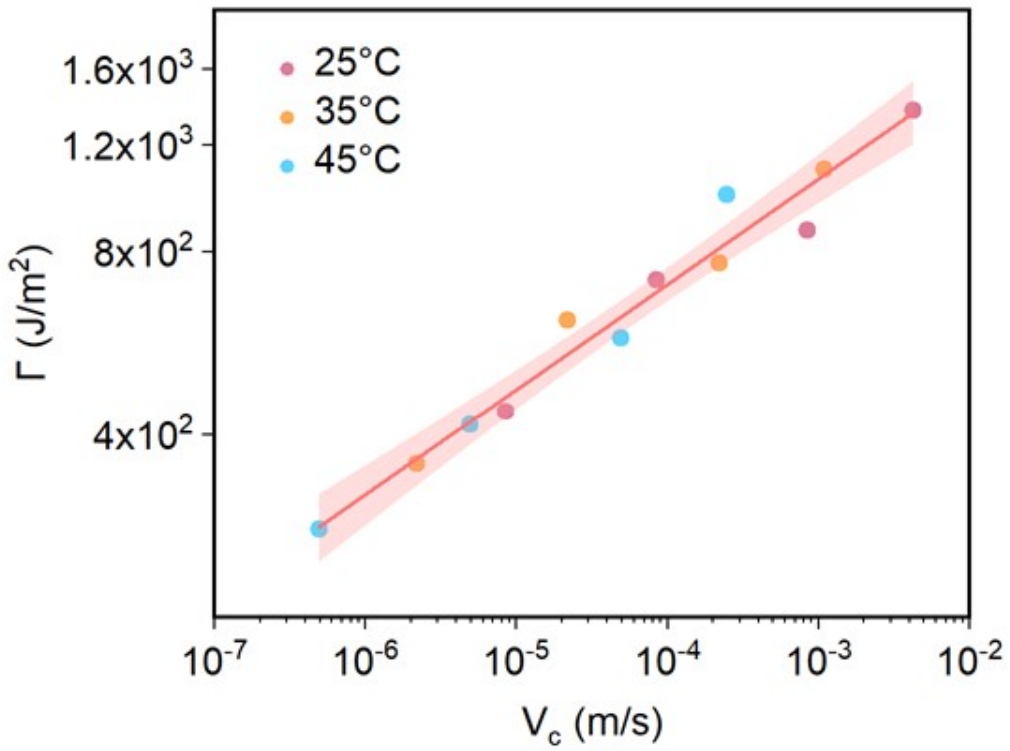

Figure S13. The same shift factors in linear rheology is applied to expand the range of the cyclic force−displacement curves of the poly (LA)/Al@Ag elastomer composites.

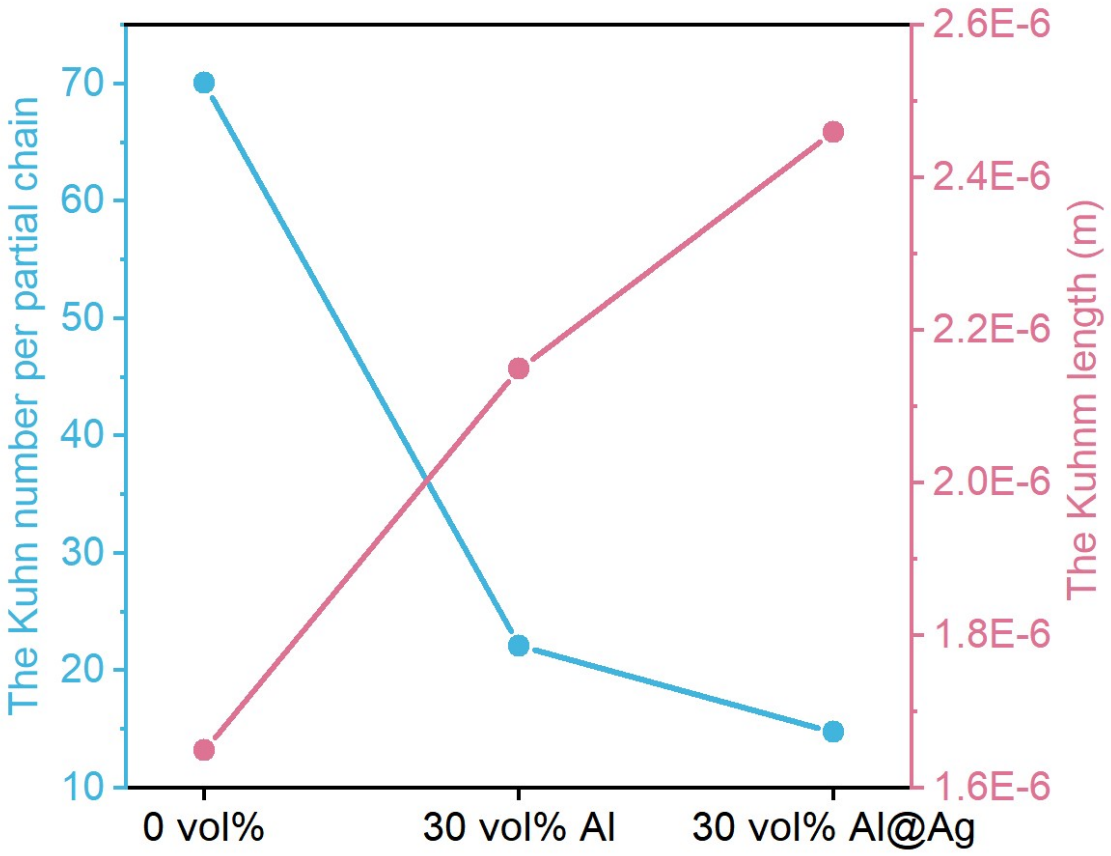

Figure S14. (A) Kuhn number Np and Kuhn length bk of the elastomer composites with different fillers.

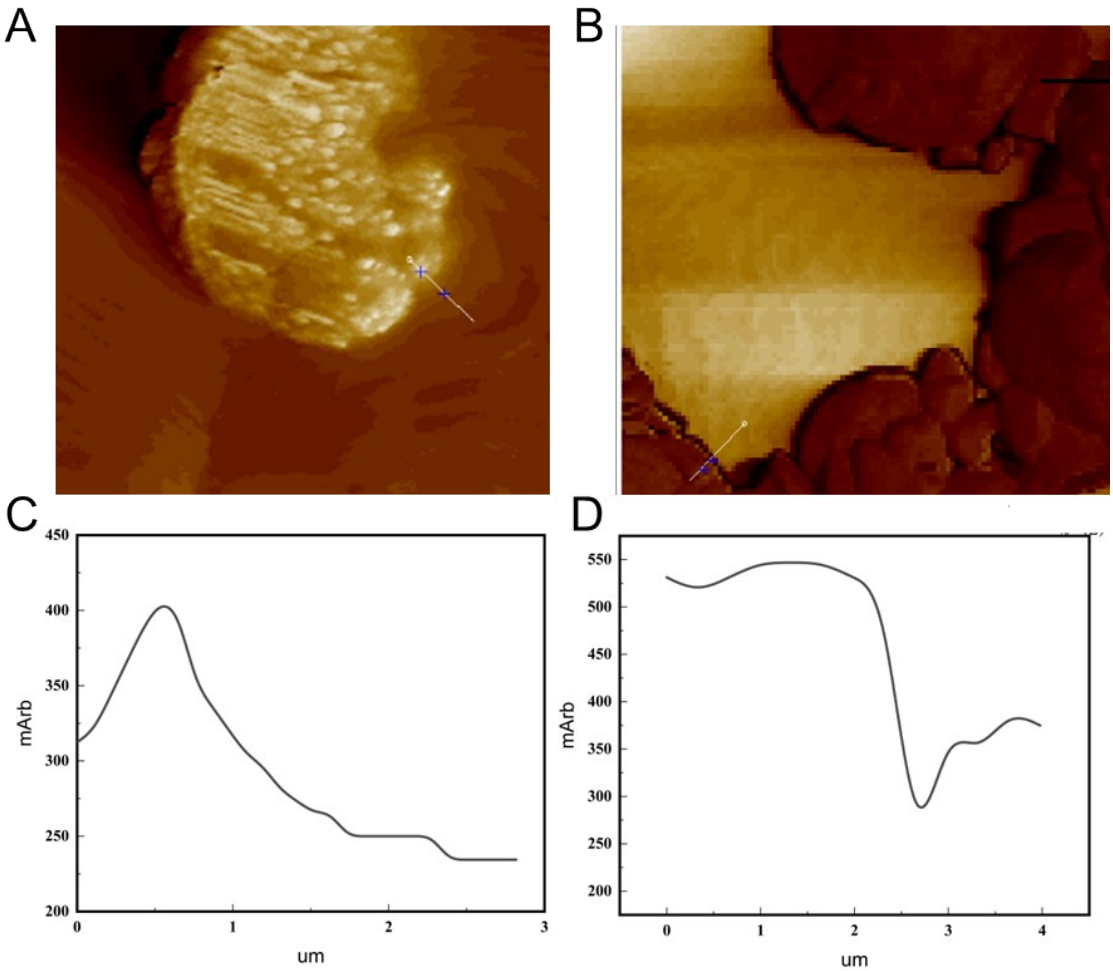

Figure S15. (A) The AFM image of the poly (LA)/ Al@Ag. (B) The AFM image of the poly (LA)/ Al. (C) The modulus change diagram is obtained by linear scanning of the scribed part of Figure A. (D) The modulus change diagram is obtained by linear scanning of the scribed part of Figure B.

$G_x = \rho RT/M_x$					
Sample	G_x	ρ	R	T	M_x
30 vol% Ag@Al	20300	2.017	8.314	298.15	22400
30 vol% Al	17115	1.689	8.314	298.15	231119

Table 1. Calculation of crosslinking density by platform modulus.